Climate variability-induced uncertainty in mid-Holocene atmosphere-ocean-vegetation feedbacks

J. Otto,[1,2] T. Raddatz,[1] and M. Claussen[1,3]

Received 21 October 2009; revised 6 November 2009; accepted 12 November 2009; published 11 December 2009.

[1] Previous modelling studies have shown that the response of the ocean and the vegetation to mid-Holocene insolation feeds back on the climate. There is less consensus, however, on the relative magnitude of the two feedbacks and the strength of the synergy between them. This discrepancy may arise partly from the statistical uncertainty caused by internal climate variability as the common analysis period is only about a century. Therefore, we have performed an ensemble of centennial-scale simulations using the general circulation model ECHAM5/JSBACH-MPIOM. The direct atmospheric response and the weak atmosphere-vegetation feedback are statistically robust. The synergy is always weak and it changes sign between the ensemble members. The simulations, including a dynamic ocean, show a large variability at sea-ice margins. This variability leads to a sampling error which affects the magnitude of the diagnosed feedbacks. **Citation:** Otto, J., T. Raddatz, and M. Claussen (2009), Climate variability-induced uncertainty in mid-Holocene atmosphere-ocean-vegetation feedbacks, *Geophys. Res. Lett.*, *36*, L23710, doi:10.1029/2009GL041457.

1. Introduction

[2] The mid-Holocene climate, 6000 years before present, is of particular interest to the understanding of the Earth System and abundant palaeoclimatic proxy records cover this period. Some boundary conditions of the climate system can be constrained accurately, in particular the variations in the Earth's orbit. These led to an increase of insolation during summer and the beginning of autumn, and to a decrease during winter compared to present day. The impact of this change in insolation on northern latitude climates has been intensively studied [e.g., *Wohlfahrt et al.*, 2004; *Braconnot et al.*, 2007; *Otto et al.*, 2009]. It has been shown that both ocean and vegetation feedbacks as well as their synergy modify the seasonal climate response to mid-Holocene insolation considerably. However, there is no agreement on the relative magnitude of the two high-latitude feedbacks, and the strength of the synergy between them. Thus, we perform several sets of simulations with a General Circulation Model (GCM) to investigate, if this discrepancy is related to internal model variability, which may affect the magnitude of the estimated feedbacks.

[3] Previous studies on the impact of feedbacks on mid-Holocene climate have been performed with Earth system Models of Intermediate Complexity (EMICs) and GCMs. A study with the EMIC CLIMBER-2 showed that the synergy between the atmosphere-ocean and atmosphere-vegetation feedback leads to an annual mid-Holocene warming [*Ganopolski et al.*, 1998]. Studies with GCMs either indicate a strong atmosphere-vegetation feedback [*Wohlfahrt et al.*, 2004; *Gallimore et al.*, 2005] or that the most important modification of the climate response is related to the atmosphere-ocean feedback [*Otto et al.*, 2009] at the high latitudes. These divergent results may be ascribed to differences in the structure and parameterisation of the models as well as to the setup of the simulations. On the other hand, models exhibit internal variability due to nonlinearities in the model physics and dynamics [*Murphy et al.*, 2004]. Therefore, the question arises how much of the differences among the models can be attributed to sampling variability. Commonly, experiments are spun up until the climate trends are small, then the last 100 to 200 years are analysed [*Braconnot et al.*, 2007]. Analysing a period of this length may not account for long-term climate variability, thus introducing uncertainties in the diagnosed feedbacks. To estimate this statistical uncertainty caused by the model's internal variability, we prolonged the simulations and repeated the factor-separation technique of the existing mid-Holocene feedback study by *Otto et al.* [2009] five times.

2. Setup of Model Experiments

[4] We performed several sets of simulations with the atmosphere-ocean GCM ECHAM5-MPIOM [*Jungclaus et al.*, 2006] including the land surface scheme JSBACH [*Raddatz et al.*, 2007] with a dynamic vegetation module [*Brovkin et al.*, 2009]. The experiment setup was designed to follow the factor-separation technique by *Stein and Alpert* [1993]. For this reason, we performed four pre-industrial climate simulations, 0kAOV, 0kAO, 0kAV, 0kA and four mid-Holocene climate simulations, 6kAOV, 6kAO, 6kAV, 6kA. The capital letters indicate the components which are run interactively (A = atmosphere, O = ocean, V = vegetation). More details about the simulations are given by *Otto et al.* [2009].

[5] We calculated the contribution of each Earth system component to the mid-Holocene climate as follows:

$$\Delta AOV = 6kAOV - 0kAOV \quad (1)$$

$$\Delta A = (6kA - 0kA) \quad (2)$$

[1]Max Planck Institute for Meteorology, Hamburg, Germany.
[2]International Max Planck Research School on Earth System Modelling, Hamburg, Germany.
[3]Meteorological Institute, University of Hamburg, Hamburg, Germany.

0094-8276/09/2009GL041457

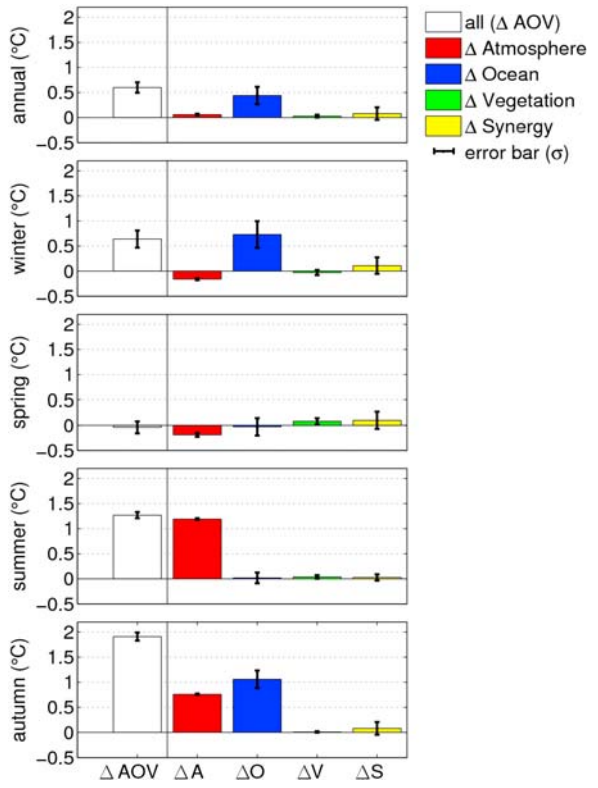

Figure 1. Contribution of factors to mean air-temperature (north of 40°) over five 120-year analysis periods. The error bar indicates one standard deviation. Note: The length of the seasons differs between 0k and 6k, as we define the seasons by astronomical dates. Thus, the annual mean is not the linear average of the seasonal means.

$$\Delta V = (6kAV - 0kAV) - (6kA - 0kA) \quad (3)$$

$$\Delta O = (6kAO - 0kAO) - (6kA - 0kA) \quad (4)$$

$$\Delta S = \Delta AOV - \Delta A - \Delta O - \Delta V \quad (5)$$

ΔAOV includes all feedbacks and synergistic effects. ΔA is the response of the atmosphere including snow cover, soil moisture and leaf phenology. The atmosphere-vegetation feedback ΔV is driven by the distribution of vegetation types and deserts. ΔO presents the atmosphere-ocean feedback including sea ice. ΔS describes the synergy between the atmosphere-vegetation and atmosphere-ocean feedback.

[6] We prolonged the simulations in order to repeat the factor separation technique five times. The $0kAOV$ and $6kAOV$-simulations were run first for 1100 years, and the last 600 years were considered for the analysis. We divided these 600 years into five analysis periods of 120 years each. The other six simulations were also prolonged up to 600 years and carried out in an analogous manner to the first analysis period [see *Otto et al.*, 2009]. To get a better picture of the long-term climate variability caused by ocean dynamics, we ran the $0kAOV$ and $6kAOV$-simulations for further 1320 years.

3. Results and Discussion

[7] This study confirms that the atmosphere-ocean feedback modifies the mid-Holocene temperature signal considerably. Figure 1 depicts the annual and seasonal mean 2m-temperature signal averaged over the five analysis periods with the uncertainty given as one standard deviation (δ) in ΔAOV, ΔA, ΔO, ΔV, ΔS of the five analysis periods. The simulations including all feedbacks and synergies, ΔAOV, show an annual warming in the mid-Holocene of 0.60°C (δ = 0.11) north of 40°N. The seasonal mean air-temperature reveals an amplification of the seasonal cycle. In summer and autumn the warming reaches 1.27°C (δ = 0.06) and 1.91°C (δ = 0.08), respectively. Contrary to the insolation signal, the winter shows a warming of 0.64°C (δ = 0.17). Only the spring shows a cooling of −0.04°C (δ = 0.12) following the decrease of insolation. ΔA shows how much of the total climate response to the orbital-induced changes in insolation is ascribed to the direct atmospheric response. It shows a winter cooling of −0.16°C (δ = 0.02), a spring cooling of −0.19°C (δ = 0.04), a summer warming of 1.19°C (δ = 0.02), and an autumn warming of 0.76°C (δ = 0.01). The atmosphere-vegetation feedback ΔV is weak in all seasons. The boreal forests shifts poleward during the mid-Holocene, and through the snow-albedo feedback in spring, causes regionally an increase in temperature. Thus, only in spring ΔV leads to a slight warming of 0.08°C (δ = 0.06) counteracting the insolation changes. The atmosphere-ocean feedback ΔO shows the strongest modification of the direct climate response. It amplifies the autumn orbital signal by 1.06°C (δ = 0.17) and counteracts the cooling in winter by 0.73°C (δ = 0.27). The synergy between the atmosphere-ocean and atmosphere-vegetation feedback results in a slight warming in all seasons and leads to an annual warming of 0.08°C (δ = 0.12).

[8] The uncertainty of the mean values is given by one standard deviation (Figure 1). The values of ΔA show similar results for each analysis period and are statistically robust (max. δ = 0.04 in spring) because of the short-time memory of the atmosphere. Similarly, the weak springtime atmosphere-vegetation feedback ΔV occurs persistently in all five analysis periods (max. δ = 0.06 in spring). By contrast, factors based on simulations with a dynamic ocean (ΔAOV, ΔO, ΔS) show a large variability. This is due to the longer time scale of variations in the ocean compared to those in the atmosphere. The values of the atmosphere-ocean feedback ΔO and ΔAOV vary most between the analysis periods in comparison to the other factors. Their standard deviation is largest in winter (ΔO δ = 0.27, ΔAOV δ = 0.17). The large variability in the simulations with a dynamic ocean influences also the synergy term ΔS, so that the error bar exceeds the mean value of ΔS in all seasons, i.e. ΔS can change sign from one analysis period to the other. This can be explained by the way the synergy term is calculated. It is the difference between ΔAOV (minuend) and the sum of the three components ΔA, ΔO and ΔV (subtrahend). ΔAOV and ΔO vary with a large amplitude and independently from each other as they are calculated

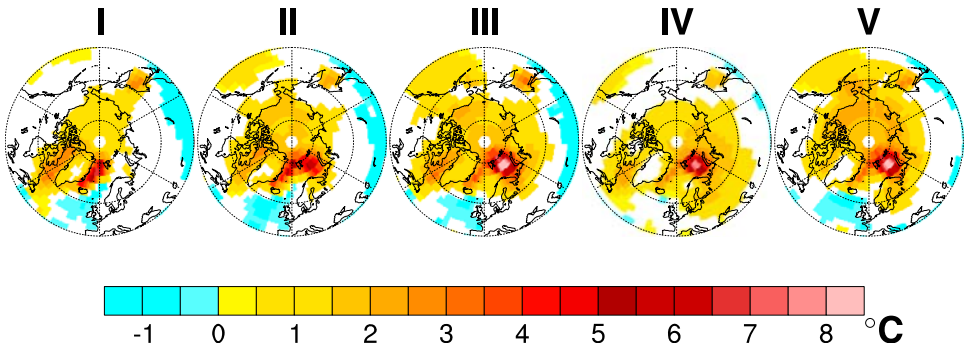

Figure 2. Winter mean temperature signal ΔAOV of the five analysis periods. Only significant values at the 99% level are displayed.

from different simulations. Thus, the subtrahend can be larger than the minuend so that the synergy term becomes negative.

[9] To analyse the large temperature variability of the simulations with a dynamic ocean more closely, we focus on the spatial temperature patterns of each analysis period. As the largest variability occurs in winter, Figure 2 depicts the spatial pattern of the winter mean temperature signal for ΔAOV. During the first two analysis periods the maximum temperature of ΔAOV occurs over the Greenland Sea with an anomaly of up to 6°C. A weaker maximum appears around the Kamchatka Peninsula. From the second analysis period onwards, the maximum temperature anomaly appears in the Barents Sea region of up to 9°C. The temperature maximum weakens slightly by 1°C in the fourth but increases in the fifth analysis period. The winter

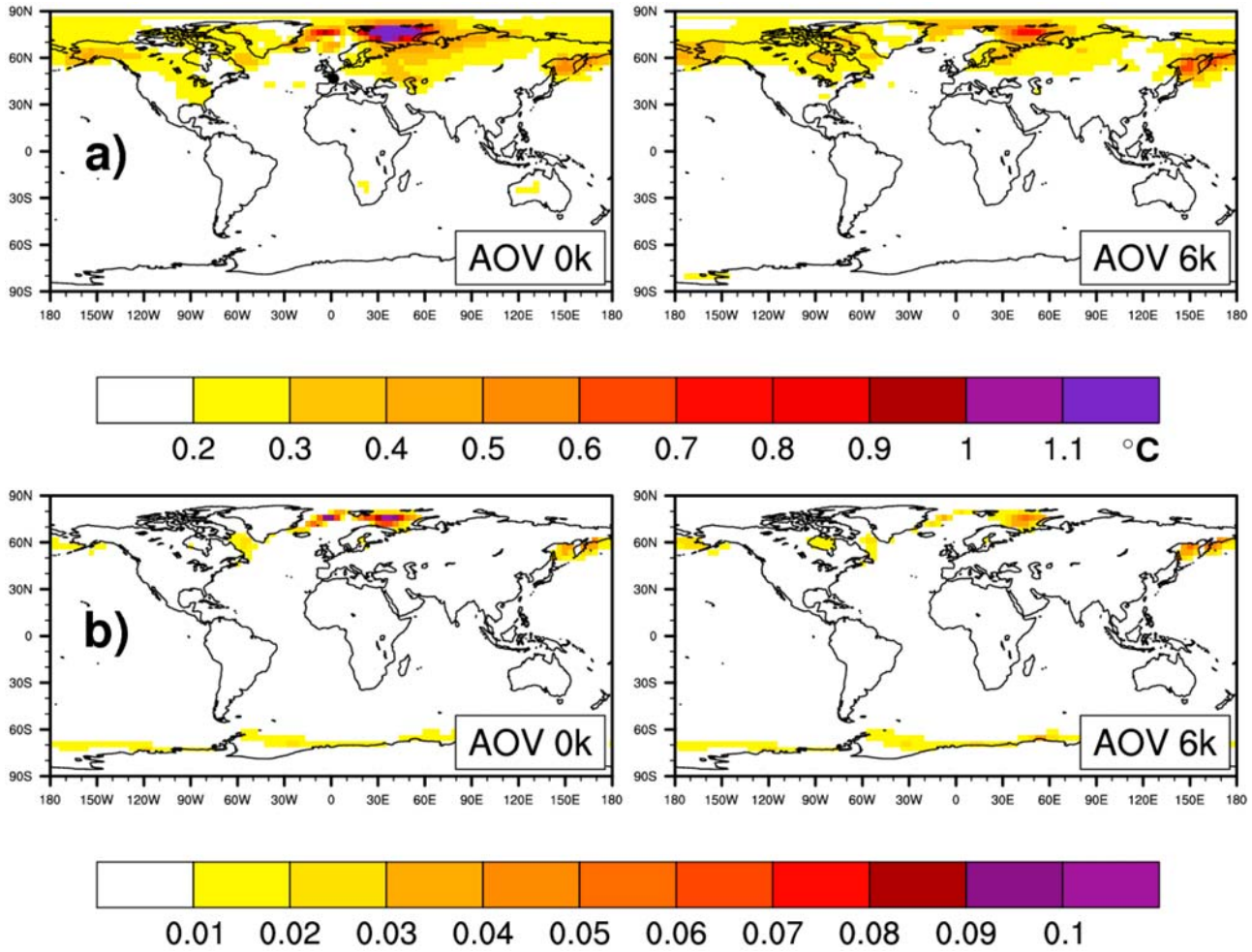

Figure 3. The standard deviation of 120-year mean winter air-temperature (n = 16) for the pre-industrial and mid-Holocene AOV-simulation (a) and the standard deviation of 120-year mean winter fractional sea-ice cover (n = 16) for the pre-industrial and mid-Holocene AOV-simulation (b).

mean temperature signals in the simulations with prescribed vegetation ΔAO (= 6kAO − 0kAO) are similar to ΔAOV (not shown).

[10] To test the robustness of these winter temperature variability estimates, we extended the simulations 0*kAOV* and 6*kAOV* for 1320 years and calculated the standard deviation of the 120-year average winter temperature and sea-ice cover for sixteen analysis periods (Figure 3). The standard deviation of the air-temperature (Figure 3a) ranges from 0.2 to 2°C. The largest variability with up to 2°C appears in the Barents Sea as well around the Kamchatka Peninsula with up to 0.8°C. The standard deviation of the fractional sea-ice cover (Figure 3b) is largest at the sea-ice margins and varies there from 0.01 to 0.1 in the Barents Sea. Figure 3 reveals that the regions of highest temperature variability match the areas of largest sea-ice variability. Furthermore, it shows that the patterns of variability with high values at the sea-ice margins are similar in 0k and 6k, and therefore statistically robust.

[11] As the winter air-temperature variability is largest at the sea-ice margins, these regions may be decisive for the long-term variations of the Northern Hemisphere temperature. To quantify the relation of these areas and the 120-year mean air-temperature north of 40°N, we selected three regions: two regions at the sea-ice margin - the Barents Sea and the region around the Kamchatka Peninsula - and the northern part of the North Atlantic (45°N–60°N). We chose the latter region because it is only marginally influenced by sea-ice. In addition, the meridional overturning circulation is considered to have the potential to introduce long-term variations to the northern latitude climate [*Ganachaud and Wunsch*, 2000]. We correlated the average temperature of each region with the average temperature north of 40°N, excluding the particular region. In winter, the Barents Sea region (r = 0.84 mid-Holocene, r = 0.70 pre-industrial) and the region around the Kamchatka Peninsula (r = 0.45 mid-Holocene, r = 0.59 pre-industrial) are strongly correlated with the temperature north of 40°N. By contrast, the North Atlantic region shows a correlation coefficient close to zero in all seasons. Hence, in our model, the regions with the strongest temperature variability influence the average winter temperature north of 40°N decisively.

[12] Our results reveal that internal climate variability affects the magnitude of the diagnosed feedbacks. This raises the question whether the variability generated in the model is comparable to natural variability. The internal variability integrated in the pre-industrial simulations (0*kAOV*, 0*kAO*) compares reasonably well with the observed annual mean temperature variability from 1949–1998 [*Delworth et al.*, 2002]. The model reproduces the large variability over continental extratropical regions. The simulated maximal variability emerges at the sea-ice margins, in particular over the Barents Sea, which is also in agreement with observations [*Divine and Dick*, 2006]. For this region, we find in our model the same strong coupling between local anomalies of atmospheric circulation and sea-ice cover (see auxiliary material) as already analysed in previous modelling studies [*Bengtsson et al.*, 2004; *Koenigk et al.*, 2009].[1] In summary, the variability generated in our model is comparable to observed variability and to the variability simulated by other models.

[13] With our model, we are able to show that the statistical uncertainty affects the magnitude of the feedbacks. The question remains how much of the previous mid-Holocene results are affected by statistical uncertainty. The results from *Ganopolski et al.* [1998] with the EMIC CLIMBER-2 are statistically robust, as CLIMBER-2 does not generate climate variability [*Petoukhov et al.*, 2000]. *Wohlfahrt et al.* [2004] and *Gallimore et al.* [2005] performed their simulations with the GCMs IPSL and FOAM-LPJ, respectively. *Wohlfahrt et al.* [2004] based their analyses on 20-year averages. *Gallimore et al.* [2005] chose analysis period of 100 and 400 years. As their analysis periods are about the same length or shorter than our 120-year analysis period, the estimated feedbacks may be affected by the statistical uncertainty. Furthermore, the studies by *Wohlfahrt et al.* [2004] and *Gallimore et al.* [2005] show a stronger vegetation feedback than our simulations. Possibly, their simulations could include a large vegetation variability. This could, in turn, enhance the ocean's variability. For example, *Notaro and Liu* [2007] showed with the GCM FOAM-LPJ that the variability in boreal forest significantly enhances the variability in SSTs over the North Pacific. Thus, large vegetation variability may affect the magnitude of the synergy. Presumably, the discrepancy of the estimated feedbacks in different GCMs can be related, in part, to internal model variability.

4. Summary and Concluding Remarks

[14] We have performed several sets of simulations to quantify how the statistical uncertainty affects the estimated atmosphere-vegetation and atmosphere-ocean feedback and their synergy to mid-Holocene insolation. Although the analysis period is long, it leads to statistical uncertainty which has different effects on the magnitude of the considered feedbacks. The atmosphere response and the weak atmosphere-vegetation feedback are statistically robust. By contrast, the factors derived from simulations with an interactive ocean are sensitive to long-term anomalies in sea-ice cover. This implies that GCM simulations with an interactive ocean should include a long spin-up time as well as a long analysis period to reduce the statistical uncertainty. This is also important with regard to model intercomparison studies. Nevertheless, this study confirms that the most important modification of the response to the orbital forcing can be related to the atmosphere-ocean interactions. The divergent results of the previous mid-Holocene studies can therefore only partly be related to internal variability.

[15] **Acknowledgments.** The authors are grateful for the constructive comments of anonymous reviewers. We would like to thank Thorben Koenigk and Nils Fischer for their helpful comments.

References

Bengtsson, L., V. A. Semenov, and O. M. Johannessen (2004), The early twentieth-century warming in the Arctic: A possible mechanism, *J. Clim.*, *17*(20), 4045–4057.

Braconnot, P., et al. (2007), Results of PMIP2 coupled simulations of the mid-Holocene and Last Glacial Maximum. Part 1: Experiments and large-scale features, *Clim. Past*, *3*(2), 261–277.

Brovkin, V., T. Raddatz, C. H. Reick, M. Claussen, and V. Gayler (2009), Global biogeophysical interactions between forest and climate, *Geophys. Res. Lett.*, *36*, L07405, doi:10.1029/2009GL037543.

[1] Auxiliary materials are available in the HTML. doi:10.1029/2009GL041457.

Delworth, T. L., R. J. Stouffer, K. W. Dixon, M. J. Spelman, T. R. Knutson, A. J. Broccoli, P. J. Kushner, and R. T. Wetherald (2002), Review of simulations of climate variability and change with the GFDL R30 coupled climate model, *Clim. Dyn.*, *19*(7), 555–574.

Divine, D. V., and C. Dick (2006), Historical variability of sea ice edge position in the Nordic Seas, *J. Geophys. Res.*, *111*, C01001, doi:10.1029/2004JC002851.

Gallimore, R., R. Jacob, and J. Kutzbach (2005), Coupled atmosphere-ocean-vegetation simulations for modern and mid-Holocene climates: Role of extratropical vegetation cover feedbacks, *Clim. Dyn.*, *25*(7–8), 755–776.

Ganachaud, A., and C. Wunsch (2000), Improved estimates of global ocean circulation, heat transport and mixing from hydrographic data, *Nature*, *408*(6811), 453–457.

Ganopolski, A., C. Kubatzki, M. Claussen, V. Brovkin, and V. Petoukhov (1998), The influence of vegetation-atmosphere-ocean interaction on climate during the mid-Holocene, *Science*, *280*(5371), 1916–1919.

Jungclaus, J. H., N. Keenlyside, M. Botzet, H. Haak, J. J. Luo, M. Latif, J. Marotzke, U. Mikolajewicz, and E. Roeckner (2006), Ocean circulation and tropical variability in the coupled model ECHAM5/MPI-OM, *J. Clim.*, *19*(16), 3952–3972.

Koenigk, T., U. Mikolajewicz, J. H. Jungclaus, and A. Kroll (2009), Sea ice in the Barents Sea: Seasonal to interannual variability and climate feedbacks in a global coupled model, *Clim. Dyn.*, *32*(7–8), 1119–1138.

Murphy, J. M., D. M. H. Sexton, D. N. Barnett, G. S. Jones, M. J. Webb, and M. Collins (2004), Quantification of modelling uncertainties in a large ensemble of climate change simulations, *Nature*, *430*(7001), 768–772.

Notaro, M., and Z. Y. Liu (2007), Potential impact of the Eurasian boreal forest on North Pacific climate variability, *J. Clim.*, *20*(6), 981–992.

Otto, J., T. Raddatz, M. Claussen, V. Brovkin, and V. Gayler (2009), Separation of atmosphere-ocean-vegetation feedbacks and synergies for mid-Holocene climate, *Geophys. Res. Lett.*, *36*, L09701, doi:10.1029/2009GL037482.

Petoukhov, V., A. Ganopolski, V. Brovkin, M. Claussen, A. Eliseev, C. Kubatzki, and S. Rahmstorf (2000), Climber-2: A climate system model of intermediate complexity. Part I: Model description and performance for present climate, *Clim. Dyn.*, *16*(1), 1–17.

Raddatz, T. J., C. H. Reick, W. Knorr, J. Kattge, E. Roeckner, R. Schnur, K. G. Schnitzler, P. Wetzel, and J. Jungclaus (2007), Will the tropical land biosphere dominate the climate-carbon cycle feedback during the twenty-first century?, *Clim. Dyn.*, *29*(6), 565–574.

Stein, U., and P. Alpert (1993), Factor separation in numerical simulations, *J. Atmos. Sci.*, *50*(14), 2107–2115.

Wohlfahrt, J., S. P. Harrison, and P. Braconnot (2004), Synergistic feedbacks between ocean and vegetation on mid- and high-latitude climates during the mid-Holocene, *Clim. Dyn.*, *22*(2–3), 223–238.

M. Claussen, J. Otto, and T. Raddatz, Max Planck Institute for Meteorology, Bundesstraße 55, D-20146 Hamburg, Germany. (juliane.otto@zmaw.de)